International Journal of Environmental Sciences
ISSN: 2229-7359
Vol. 11 No. 15s,2025
https://theaspd.com/index.php

Molecular Docking-Based Analysis Of TNNT2 Variants: A Computational Approach To Cardiomyopathy-Associated Mutations

N Ravi[1], U S H Raghavendra Prasad[2], N Sravanthi[3], M Kavitha[4]
[1,2,3,4]Department of Chemistry, University College of Science, Osmania University, Hyderabad-500007, Telangana, India.

ABSTRACT
Heritable cardiomyopathies have been strongly linked to pathogenic variants in the TNNT2 gene [1], which encodes cardiac troponin T – a critical regulatory subunit of the troponin complex within the sarcomere. These mutations compromise the normal calcium-dependent regulatory mechanism of cardiac contraction by destabilizing the structural and functional integrity of the troponin-tropomyosin complex. Depending on their specific location and biochemical nature, TNNT2 mutations [2] may lead to altered calcium sensitivity, impaired contractile signaling, or sarcomeric disorganization. Such molecular perturbations are associated with divergent clinical outcomes, including hyper contractile phenotypes typical of hypertrophic cardiomyopathy [3] and hypo contractile states characteristic of dilated cardiomyopathy [4]. These changes not only reduce cardiac efficiency but also contribute to maladaptive remodeling, promoting arrythmogenic substrates and progressive cardiac dysfunction. In this investigation, we employ advanced computational strategies-specifically molecular docking and virtual screening-to identify novel small-molecule modulators that can potentially rectify the structural and functional deficits caused by disease-associated TNNT2 mutations.
Keywords: *TNNT2-Troponin T2, Hypertrophic Cardiomyopathy, arrythmogenic, Dilated Cardiomyopathy*

INTRODUCTION

Cardiomyopathy encompasses a heterogeneous group of myocardial disorders characterized by structural and functional abnormalities in the absence of coronary artery disease, hypertension [4], or valvular pathology sufficient to explain the phenotype. It is broadly classified into hypertrophic, dilated, and restrictive and arrhythmogenic subtypes, each associated with distinct clinical manifestations and genetic underpinnings. At the molecular level, cardiomyopathies often result from mutations in genes encoding sarcomeric or cytoskeletal proteins, leading to impaired contractility, ventricular remodeling, and arrhythmias [5]. The condition poses a significant risk of heart failure and sudden cardiac death, necessitating early diagnosis and a molecularly guided approach to treatment and risk stratification.

The TNNT2 protein (Cardiac troponin T) integrates with tropomyosin and troponin (TNNI3) [6] to regulate calcium-mediated contraction of cardiac muscle through its association with actin filaments. Mutations in TNNT2 [7] disrupt this regulatory mechanism, leading to altered calcium sensitivity, sarcomeric instability [8], and impaired contractile dynamics [9]. These molecular dysfunctions contribute to the onset of cardiomyopathies, primarily in the form of hypertrophic or dilated phenotypes [10]. The Figure 1 illustrates the mechanistic transition from a structurally stable troponin complex to a dysfunctional state caused by genetic variation, establishing a direct link between TNNT2 mutations and cardiac disease progression.

Figure A. Schematic illustration of TNNT2 mutation causing Cardiomyopathy

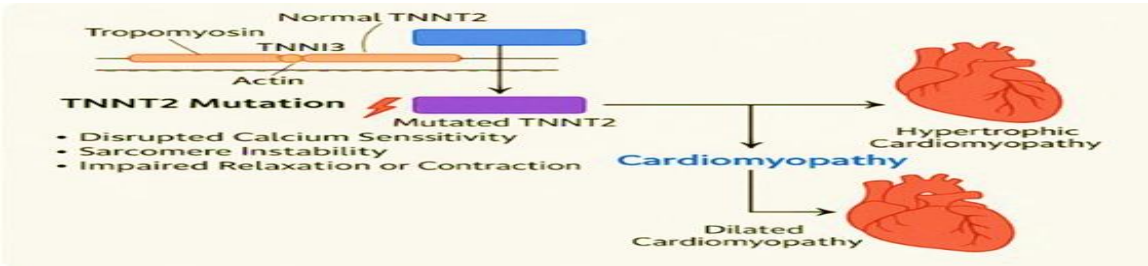

METHODOLOGY

Retrieval of Protein Data and 3D structure information

The UniProt database [11] is a cornerstone resource in the field of bioinformatics offering an extensive and meticulously curated collection of protein sequences and associated annotations. It aggregates information from reliable sources such as Swiss-Prot, TrEMBL, and PIR, making it indispensable for biological and biomedical studies. UniProt includes a wide array of details about protein function, structural characteristics, sequence attributes, and taxonomic data.Similarly, the Protein Data Bank (PDB) [12] is an openly accessible repository containing three-dimensional structures of biological macromolecules, including proteins and nucleic acids. Data in the PDB is contributed by researchers around the world and is primarily derived from the experimental methods like X-ray crystallography, nuclear magnetic resonance (NMR) spectroscopy, and cryo-electron microscopy. The PDB plays a pivotal role in the field of structural biology and supports advance in drug design and computational biology.

Structural Validation

To ensure the quality of the predicted 3D structure of the TNNT2 protein, the model underwent stereochemical evaluation using the PROCHECK tool [13] [14], which is accessible through the SAVES [15] [16] (Structural Analysis and Verification Server) suite. A Ramachandran plot [17] was generated to assess the distribution of backbone dihedral angle among amino acids, providing insight into structural accuracy. Additionally, energy-based assessments were conducted using the ProSA tool [18], which calculated a Z-score to compare the existing 3D structure reliability against the other experimentally determined protein structures.

Determination of Active sites of the Protein

Accurately pinpointing a protein's active site is crucial for elucidating its biological role and plays a fundamental part in the rational design of drugs based on molecular structure. To achieve this, computational techniques are often employed to forecast potential ligand-binding regions within the three-dimensional architecture of the protein. Tools such as CASTp [19] and SiteMap [20], included in the Schrödinger software suite, and are widely utilized to identify hydrophobic cavities and other structural features favorable for ligand attachment.

Structure-Based Virtual Screening via Molecular Docking

Molecular docking is a widely adopted computational strategy used to predict the interaction between small molecule ligands and biological targets, often proteins.

This approach is integral to the drug discovery process, enabling identification of compounds that may elicit specific biological effects through binding. The effectiveness of docking relies on a deep understanding of the target protein's structural features and energetic landscape.

In the context of this research, 3D structure of TNNT2 was employed for virtual screening using GLIDE (Grid-Based Ligand Docking with Energetics), version. This tool stimulates ligand binding and estimates interaction strength through a hierarchical screening workflow. Docking parameters were set with a van der Waals scaling factor of 1.0 and a partial charge cutoff of 0.25. A cubic docking grid of size X Å × Y Å × Z Å was centered on the active site.

Ligands were sourced from the CMNPD (Comprehensive Marine Natural Products Database) [21]-[23] library. These molecules were processed in Maestro (v9.1, Schrodinger, LLC, New York) using the LigPrep Module (version 4.0) to generate 3D structures at physiological pH (7.0 ± 2.0), applying the OPLS_2004 force field. Various stereoisomers, tautomer's, and ionization states were generated using default parameters to ensure optimal conformational diversity.

Following this, flexible docking was conducted in stages: initial screening with High Throughput Virtual Screening (HTVS) mode filtered out low-affinity ligands; the top 10% of hits progressed to Standard Precision (SP) docking for detailed scoring. Finally, the best candidates underwent Extra Precision (XP) docking for the highest accuracy in pose prediction. The docked complexes were refined based on bond geometry and scored using the GLIDE scoring algorithm. Top-scoring ligands were then evaluated for their pharmacokinetic properties through ADMET analysis.

ADMET evaluation

A thorough assessment of Absorption, Distribution, Metabolism, Excretion, and Toxicity (ADMET) [24] [25] characteristics is a crucial step in early drug discovery, as it plays an essential role in determining the feasibility of clinical development and the potential for market success of candidate compounds. Ligand molecules identified through virtual screening and molecular docking-particularly those showing strong binding affinity to TNNT2-undeerwent ADME analysis using the QikProp [26] module integrated within the Schrödinger software suite. To evaluate toxicity risks and ease of clinical synthesis, the ProTox 3.0 [27] [28] web-based platform was utilized. Ligands with optimal pharmacokinetic and safety profiles were prioritized as viable therapeutic leads for cardiomyopathy treatment.

1. RESULTS AND DISCUSSION

Protein Structure Retrieval, Analysis, and Validation

a) Acquisition of the TNNT2 protein Structure

The three-dimensional structure of the TNNT2 protein was obtained from the Protein Data Bank (PDB) using the accession code 1J1D_B. This particular model was selected due to its high resolution of 2.61 Å, completeness, and relevance for molecular docking applications. Prior to initiating docking procedures, the protein structure was preprocessed using the Schrodinger software suite. This involved removing non-essential components such as water molecules, unrelated chains, and heteroatoms. To prepare the structure for computational studies, polar hydrogen atoms were added, and Kollman charges were assigned, ensuring an optimal conformation for subsequent in silico analysis.

b) Structure Validation

Figure 2.1 Ramachandran Plot obtained using SAVES Server

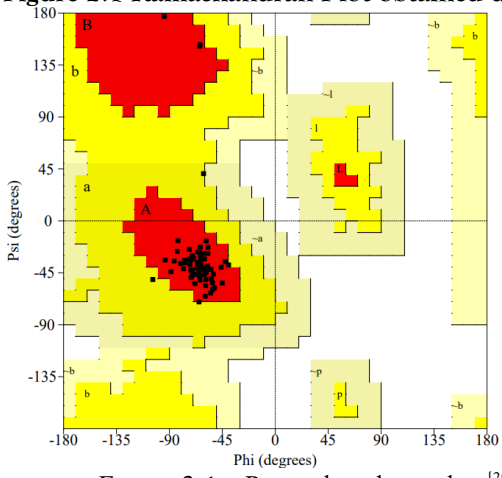

Plot statistics

Residues in most favoured regions [A,B,L]	64	94.1%
Residues in additional allowed regions [a,b,l,p]	4	5.9%
Residues in generously allowed regions [~a,~b,~l,~p]	0	0.0%
Residues in disallowed regions	0	0.0%
Number of non-glycine and non-proline residues	68	100.0%
Number of end-residues (excl. Gly and Pro)	2	
Number of glycine residues (shown as triangles)	0	
Number of proline residues	0	
Total number of residues	70	

Based on an analysis of 118 structures of resolution of at least 2.0 Angstroms and R-factor no greater than 20%, a good quality model would be expected to have over 90% in the most favoured regions.

Figure 2.1. Ramachandran plot [29] [30] of TNNT2 reveals 94.1% of residues positioned in the most favored regions, which is indicative of a highly stereochemically accurate model. Typically, models surpassing 90% in these regions are considered structurally robust.

To ensure the structural validity of the TNNT2 protein model, stereochemical analysis was conducted using a Ramachandra plot (Figure 2.1). The results indicated that 94.1% of the residues were located in energetically favorable regions, affirming the high stereochemical accuracy of the protein.

Figure 2.2 ProSA the Z-Score of the TNNT2 protein

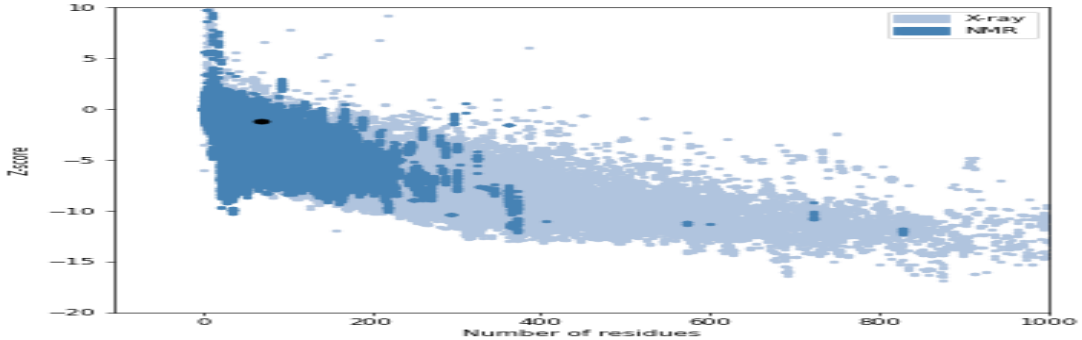

Figure 2.2 The Z-score [31] from ProSA analysis was found to be -1.16, which is well, within the range expected for native protein structures determined by X-ray crystallography or NMR. This score reflects a strong resemblance to experimentally validated protein structures.The ProSA-web server was also used to assess both global and local quality (figure 2.3). By comparing the existing structure against proteins of similar length in the Protein Data Bank (PDB), the tool confirmed the reliability of the TNNT2 structure.

Figure 2.3 Local Model Quality of the TNNT2 protein

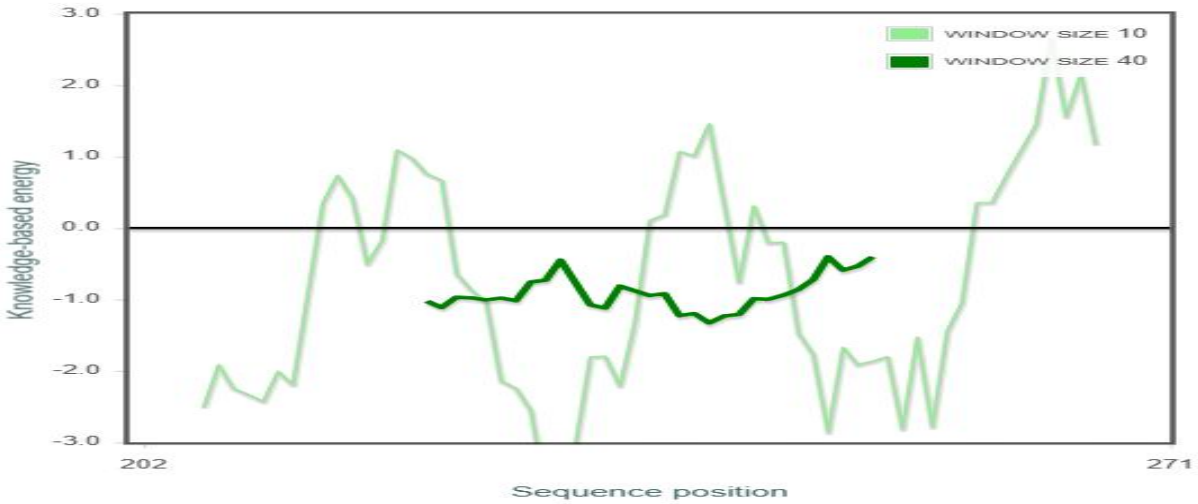

Figure 2.3 Local quality evaluation using the ProSA energy plot [32] employed knowledge-based scoring methods. The plot uses two window sizes (10 and 40 residues) to detect structural inconsistencies. Most energy values fell below the baseline, suggesting local regions adopt stable, energetically favorable conformities.

1. **Secondary Structure Characterization**

Structure visualization confirms that the TNNT2 protein is composed of α helices. Secondary structure analysis performed using PDBsum server [33] provides a schematic overview of these elements and their arrangement within the protein (Figure 3.1). Two methods of representation of protein secondary structure first one is in α helices and second one is cylindrical mode. The figure (3.1) shows two α helices which are 203 to 222 and from 225 to 270 amino acid.

Figure 3.1 The 3D ribbon representation of TNNT2 shows the protein consists of 2 α helices.

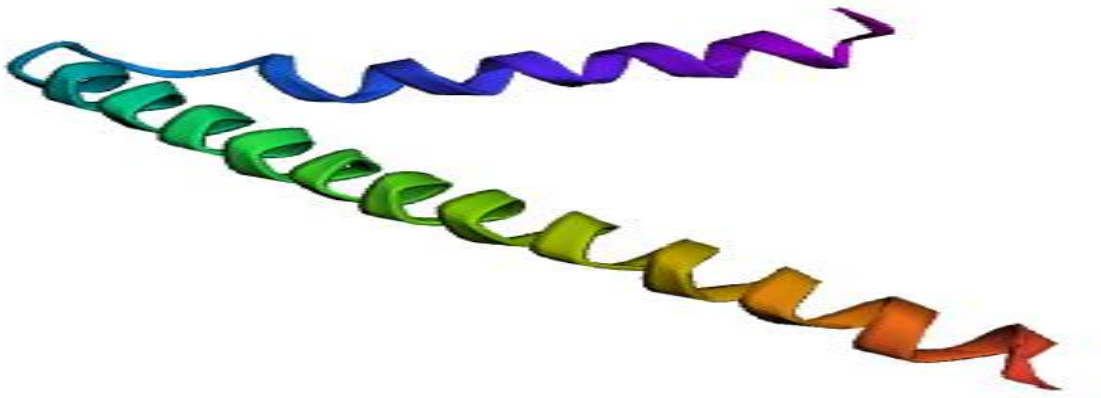

1.2. Cylindrical representation of protein using PDBsum server

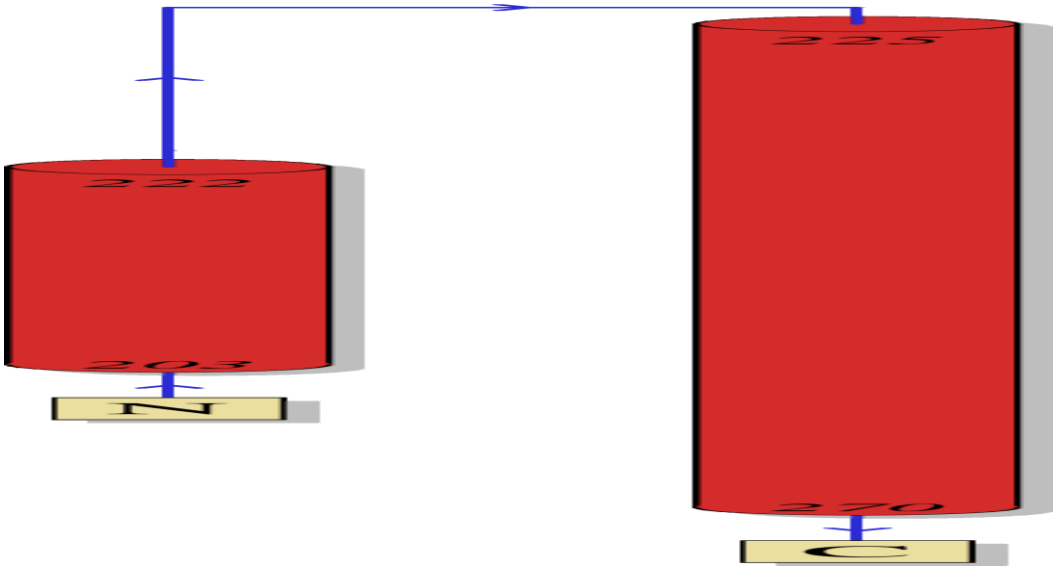

2. Active Site Identification via Computational Approaches

Computational methods, including CASTp and SiteMap, were employed to predict possible binding regions within the TNNT2 structure. CASTp used both Connolly's molecular surface and Richard's solvent-accessible surface to identify hydrophobic cavities (Table 4.1). These pockets are located in areas likely to be functionally relevant.

Table 4.1 Putative Active sites confirmed using CASTp and SiteMap

S. NO.	Active site server	Volume of the active site (Å)	Amino acids From to To
1	CASTp	27.321	216,217,220,221, 232,236
2	SiteMap	18.522	215, 221, 222, 226

CASTp identified prominent cavities, which were supported by SiteMap's prediction of similar hydrophobic regions, suggesting that the identified regions serve as potential ligand-binding sites for TNNT2 protein.

3. Structure-Based Virtual Screening and Molecular Docking

Structure-based virtual screening (SBVS) was conducted to discover novel ligands that may bind to TNNT2. A docking grid of dimensions 23 Å × 80 Å × -4.95 Å was placed over the identified active site. Ligands from the Comprehensive Marine Natural Products Database (CMNPD) were prepared using Schrodinger's LigPrep, which optimized their geometry, protonation states, and tautomerism.

Approximately 30,000 molecules were processed and generated 45,000 unique structures. These were subjected to hierarchical docking using Glide's HTVS, SP, and XP protocols. From this, 15 ligands demonstrated significant binding affinities, with the top five selected based on Glide score (Table 5.1).

Table 5.1 Binding interactions of ligands with TNNT2 protein

S.NO.	Ligand	Glide Score	Glide Energy (kcal/mol)	Hydrogen Bond with Amino Acid	Hydrogen Bond Distance (Å)
L1	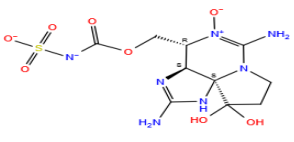	-7.423	-55.946	L1-ARG216 (1) L1-ARG216(2) L1-LYS232 L1-LYS217	2.40 2.30 1.72 1.57

L2	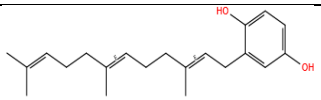	-7.333	-54.666	L2-GLN257 L2-LEU250(A)	1.79 2.61
L3	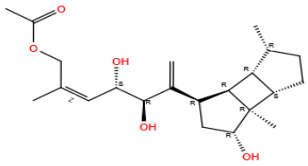	-6.823	-49.560	L3-GLU246 L3-LEU243 L3-LYS247	1.71 1.85 1.93
L4	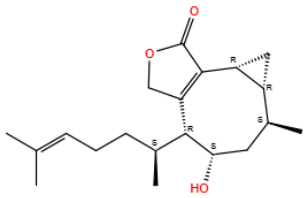	-5.423	-45.946	L4-ARG216	1.88
L5	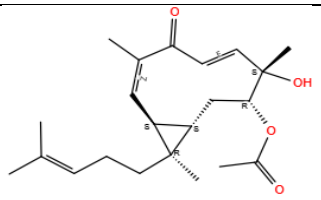	-5.216	-43.265	L5-ARG216	1.63

Hydrogen bond interactions were observed, with distances ranging between 1.57 Å and 2.40 Å (Table 5.1). Visualization performed using Accelrys Discovery Studio [34] [35] confirmed stable and specific interactions with TNNT2 protein (Figure 5.1).

Figure 5.1 Ligand (L1 –L5) interaction with TNNT2 protein

Ligand 1 – TNNT2 Interaction

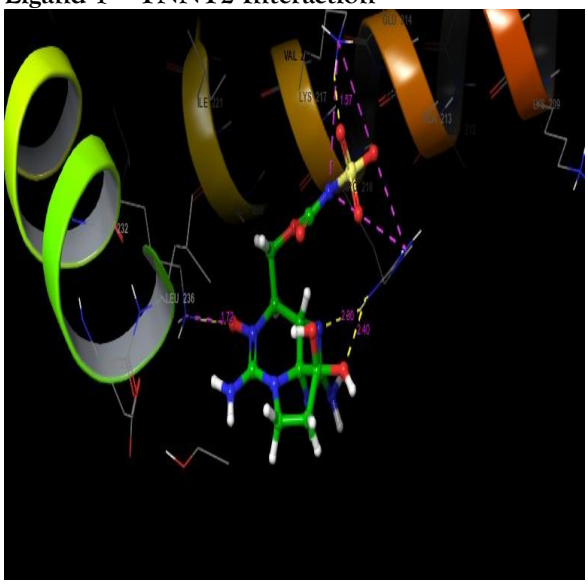

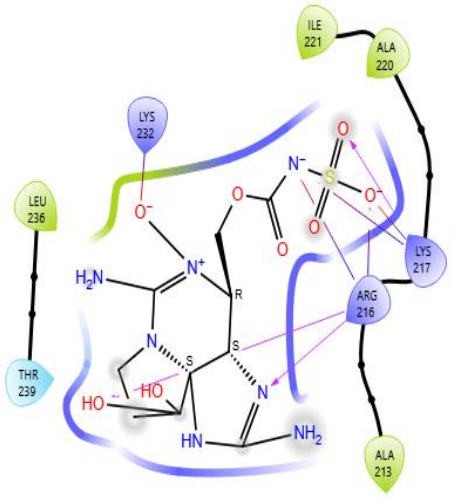

Ligand 2 – TNNT2 Interaction

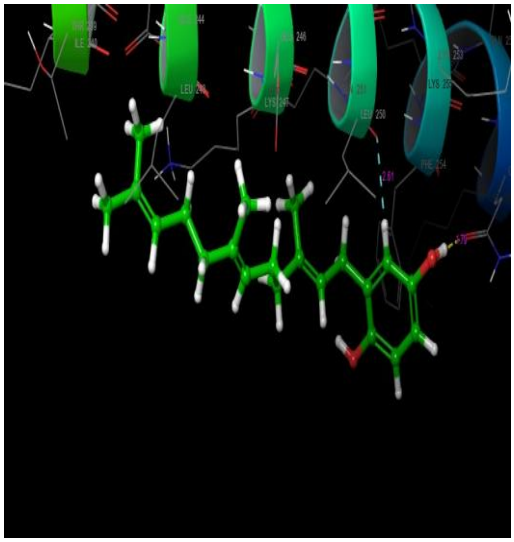

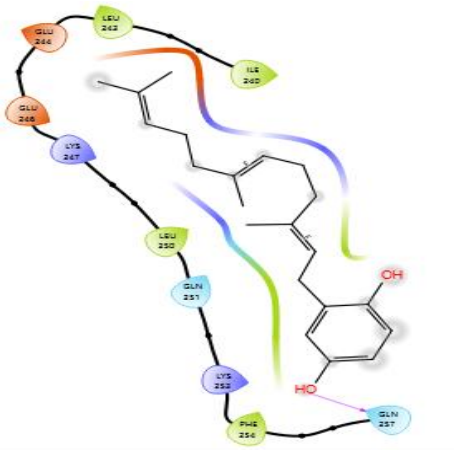

Liagnd 3 – TNNT2 Interaction

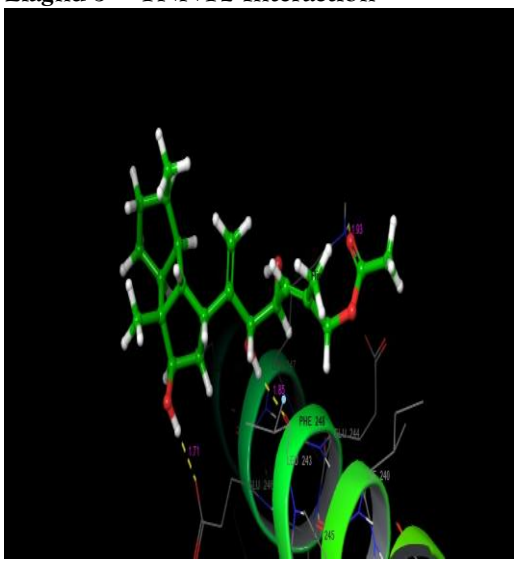

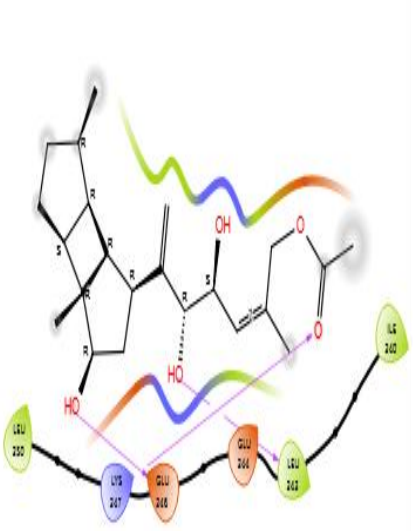

Ligand 4 – TNNT2 Interaction

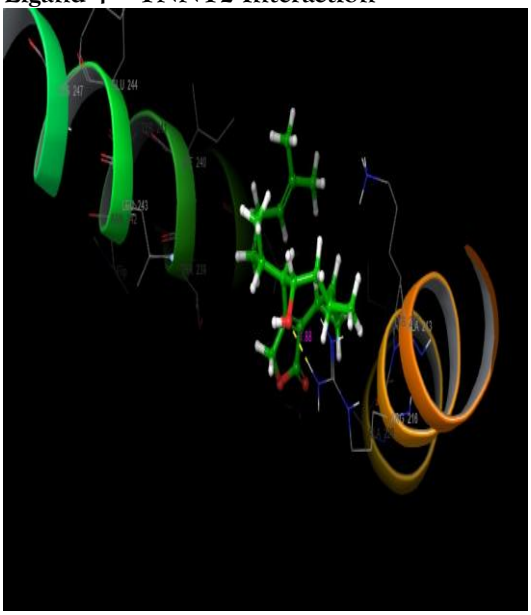

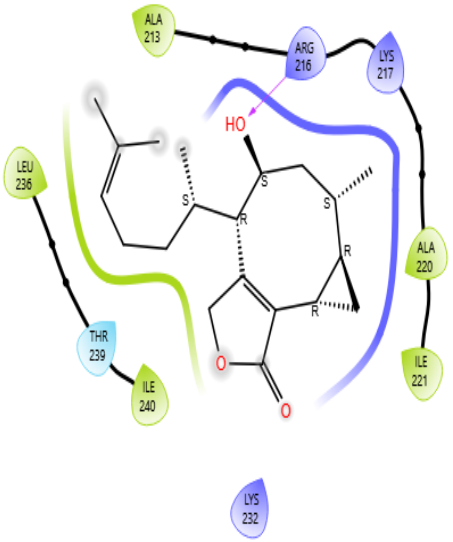

Liagnd 5 – TNNT2 Interaction

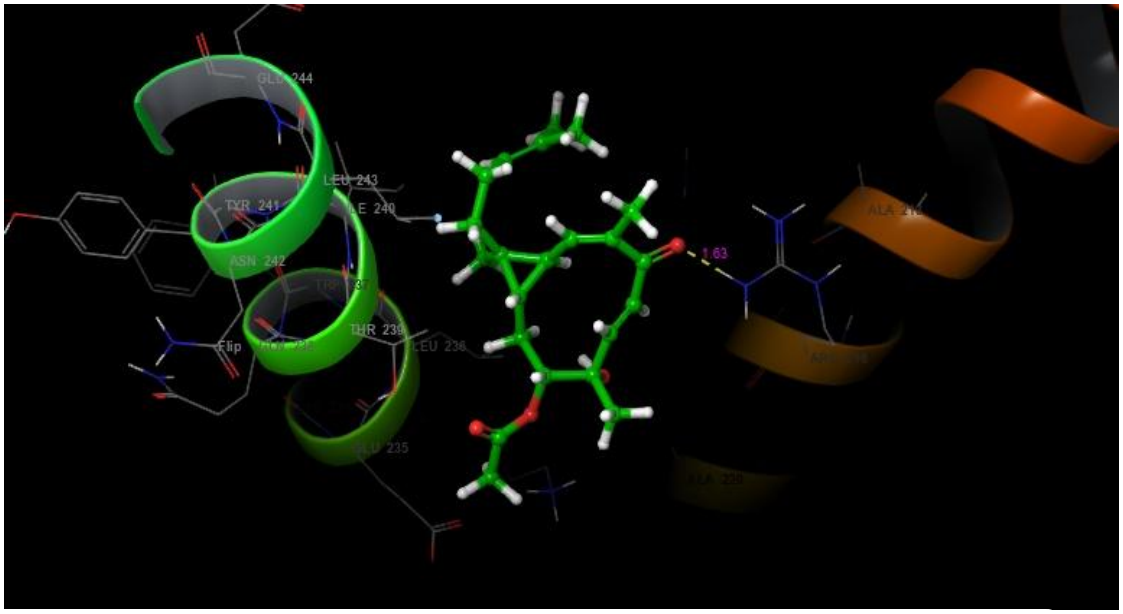

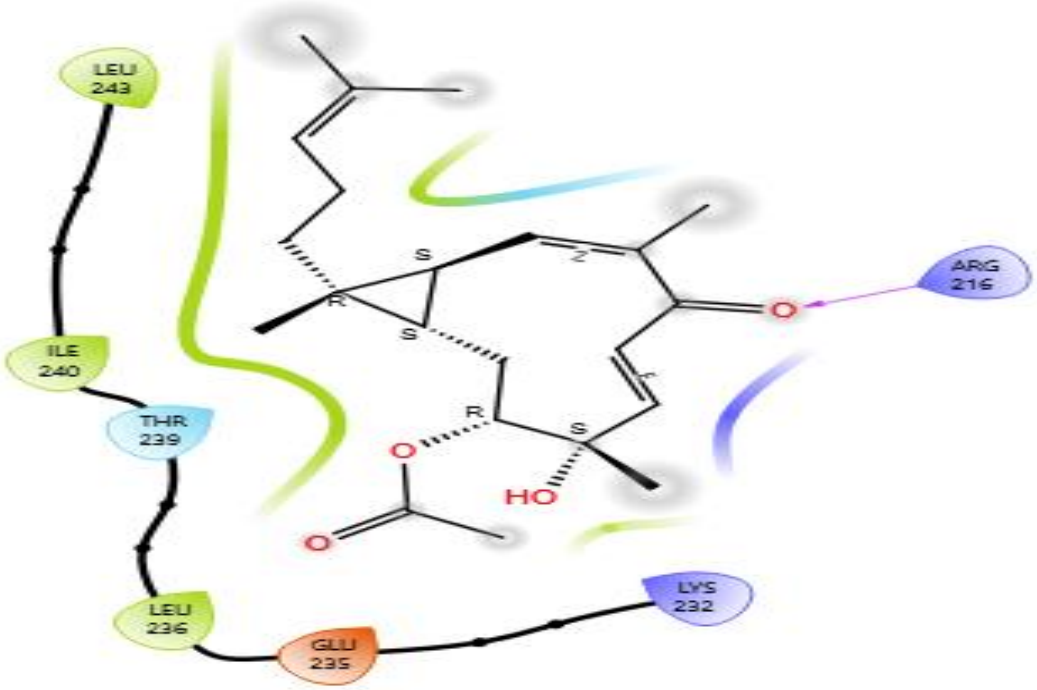

4. ADMET Evaluation (Absorption, Distribution, Metabolism, Elimination, and Toxicity)

a) Physicochemical Properties

Drug-likeness and pharmacokinetics of top-ranked molecules were evaluated using QikProp (Schrodinger Suite) [36] [37]. All compounds adhered to acceptable ranges from molecular weight (≤ 395.346), donor (≤ 4), and acceptors (≤ 10), suggesting favorable physicochemical properties (Figure 6.1).

b) Pharmacokinetic Profile

Human oral absorption (HOA) ranged from 91.404 % to 100 %, indicating excellent oral bioavailability. Water solubility (QPlogS) values remained within the acceptable range of -2.021 to -6.0. Caco^{-2} permeability (QPPCaco) values ranged from 410.376 to 1509.866, suggesting good intestinal absorption. Protein binding affinities (QPlogKhsa) were between -0.92 to 1.16, and blood-brain barrier permeability (QPlogBB) ranged from -3.00 to -0.403, indicating low risk of CNS toxicity.

Predicted CNS activity scores were negative, supporting minimal neurotoxic potential. Cardiac safety was supported by acceptable hERG inhibition values (-5.979 to -1.761) shown in Figure 6.2.

c) **Drug-Likeness Properti** All candidate molecules complied with Lipinski's Rule of Five [38] and Jorgenson's Rule of Three [39], which are commonly used to assess drug-likeness. The lipophilicity (QPlogPo/w) values were in the range of -1.438 to 5.746.

6.1. The Permissible ADME properties

S. No.	Descriptor	ADME property	permissible ranges or recommended value
1	**CNS**	Predicted central nervous system activity on -2 to +2 scale	–2 (inactive) to +2 (active)
2	**mol_MW**	Molecular weight of the molecule	130 to 725
3	**DHB**	Estimated number of hydrogen bonds that would be donated by the solute to water molecules in an aqueous solution	0 to 6
4	**AHB**	Estimated number of hydrogen bonds that would be accepted by the solute from water molecules in an aqueous solution	2 to 20
5	**QPPCaco**	Predicted apparent Caco-2 cell permeability in nm/sec	<25 poor, >500 great
6	**QPlogPw**	Predicted water/gas partition coefficient.	4.0 – 45.0
7	**QPlogPo/w**	Predicted octanol/water partition coefficient	–2.0 – 6.5
8	**QPlogS**	Predicted aqueous solubility, log S. S in mol dm^{-3}	–6.5 – 0.5
9	**QPlogKhsa**	Prediction of binding to human serum albumin	–1.5 – 1.5
10	**QPlogHERG**	Predicted IC_{50} value for blockage of HERG K^+ channels	Below +5.0
11	**QPlogBB**	Predicted blood / partition coefficient	–3.0 – 1.2
12	**% human oral absorption**	Predicted human oral absorption on 0 to 100% scale	>80% is high <25% is poor
13	**Rule Of Five**	Number of violations of Lipinski's rule of five	maximum is 4
14	**Rule Of Three**	Number of violations of Jorgensen's rule of three	maximum is 3
15	**Synthetic feasibility**	Predicted synthetic feasibility: on scale of 1 to 10;	0 = high feasibility 10 = least feasible
16	**Lipophilicity**	Predicted lyophilic nature of the ligand calculated from pIC50-LogP	min -6; max +3

Figure 6.2 ADME Properties of Ligands L1 to L5

Ligand Number	Physicochemical Properties				Pharmacokinetic Properties							Drug Likeness Property		
	mol_MW	donorHB	accptHB	QPlogS	HOA%	QPPCaco	QPlogKhsa	QPlogPw	QPlogBB	CNS	QPlogHERG	RuleOfFive	RuleOfThree	QPlogPo/w
D1	395.346	4	10	-2.021	100	600.423	-0.92	23.608	-3.000	-2	-1.761	2	1	-1.438
D2	314.467	2	1.5	-6.01	100	1253.915	1.16	5.426	-1.093	-2	-5.979	1	2	5.746
D3	378.508	3	7.1	-4.827	91.404	410.376	0.233	11.942	-1.454	-2	-4.679	0	0	3.021
D4	318.455	1	4.7	-3.526	100	1509.866	0.357	6.625	-0.403	0	-2.707	0	1	3.275
D5	360.492	1	4.75	-5.484	100	904.702	0.818	7.152	-0.734	-1	-3.922	0	0	4.24

d) Toxicity Assessment

To examine metabolic liabilities, the compounds were analyzed for interactions with Cytochrome P450 enzymes using Pro Tox 3.0 [40] (Figure 6.3). The results showed that several ligands either inhibited or did not inhibit key CYP450 isoforms, which is crucial for evaluating drug-drug interactions and metabolic stability and shown to be inactive towards Hepatotoxicity, and Cardiotoxicity. Overall, the identified compounds exhibited favorable drug-like profiles with reduced toxicity risks, supporting their potential as candidate therapeutics for cardiomyopathy treatment

Figure 6.3 Toxic Profile of Ligands L1 to L5 obtained from Virtual Screening.

S. NO.	LIGANDS	CYP-1A2	CYP-2C19	CYP-2C9	CYP-2D6	CYP-3A4	HEPATOTOXICITY	CARDIOTOXICITY
1	L1	INACTIVE	INACTIVE	INACTIVE	INACTIVE	INACTIVE	INACTIVE	INACTIVE
2	L2	INACTIVE	INACTIVE	ACTIVE	INACTIVE	ACTIVE	INACTIVE	INACTIVE
3	L3	INACTIVE	INACTIVE	INACTIVE	INACTIVE	INACTIVE	INACTIVE	INACTIVE
4	L4	INACTIVE	INACTIVE	INACTIVE	INACTIVE	INACTIVE	INACTIVE	INACTIVE
5	L5	INACTIVE	INACTIVE	INACTIVE	INACTIVE	INACTIVE	INACTIVE	INACTIVE

CONCLUSION:

In silico findings suggest that the screened compounds possess both high binding affinity and desirable drug-like characteristics, supporting their candidacy as lead molecules for the development of targeted therapies against the cardiomyopathy.

ACKNOWLEDGEMENT

Authors are thankful to Osmania University for providing required Computational software's.

REFERENCES

Larrañaga-Moreira, J. M., Ochoa, J. P., Peteiro-Debén, R., et al. (2025). The p. Asn271Ile variant in the TNNT2 gene is associated with low-risk late-onset hypertrophic cardiomyopathy. JACC: Heart Failure.

1. Lan, F., Talanaite, D., Wang, H., Qi, M. (2025). Generation of a human embryonic stem cell line (WAe009-A-3B) carrying homozygous TNNT2 gene knockout by CRISPR/Cas9 editing. Stem Cell Research

2.Larrañaga-Moreira, J. M., Ochoa, J. P., Peteiro-Debén, R., et al. (2025). The p. Asn271Ile variant in the TNNT2 gene is associated with low-risk late-onset hypertrophic cardiomyopathy. JACC: Heart Failure.

3.Zhou, W., Ye, D., Tester, D., Kim, C. J., et al. (2025). Re-engineered cardiac cells with R141W-TNNT2-mediated dilated cardiomyopathy. Heart Rhythm.

4.Yu, A. C. M., Sedlic, A., Singh, H., Darras, K., Clarke, B., et al. (2025). Cardiac Sarcoidosis and Troponin T-Related Cardiomyopathy. JACC: Case Reports.

5.Rosa, S. A. (2025). On the way to "image" the genotype. International Journal of Cardiology. https://www.internationaljournalofcardiology.com/article/S0167-5273(24)01248-8/abstract

6.Chumakova, O. S., Baklanova, T. N., et al. (2025). Clinical Features and Prospective Outcomes of Thin-Filament Hypertrophic Cardiomyopathy. Journal of Clinical Medicine, 14(3), 866.

7.Sehnert, A. J., Huq, A., Weinstein, B. M., Walker, C., Fishman, M., & Stainier, D. Y. R.(2002). Cardiac troponin T is essential in sarcomere assembly and cardiac contractility. Nature Genetics, 31, 106–110. https://www.nature.com/articles/ng875z

8.Hosseini Baygi, D. (2025). A biological investigation of microtubules in hypertrophic cardiomyopathy associated troponin-T (TNNT2) variants using human-induced pluripotent stem cell-derived cardiomyocytes. Simon Fraser University.
9.Nagashima, T., Miki, K., & Miyagawa, S. (2024). In vitro modelling and functional improvement of TNNT2-R141W mutant pediatric dilated cardiomyopathy. Circulation.https://www.ahajournals.org/doi/abs/10.1161/circ.150.suppl_1.4144727
10. The UniProt Consortium. (2023). UniProt: the Universal Protein knowledgebase in 2023. Nucleic Acids Research, 51(D1), D523–D531. https://doi.org/10.1093/nar/gkac1052
11. Berman, H. M., Westbrook, J., Feng, Z., et al. (2000). The Protein Data Bank. Nucleic Acids Research, 28(1), 235–242. https://doi.org/10.1093/nar/28.1.235
12. Laskowski, R. A., MacArthur, M. W., Moss, D. S., & Thornton, J. M. (1993). PROCHECK: a program to check the stereochemical quality of protein structures. Journal of Applied Crystallography, 26(2), 283–291. https://doi.org/10.1107/S0021889892009944
13. Morris et al. (1992) — Validation of Protein Models Using PROCHECK Morris, A. L., MacArthur, M. W., Hutchinson, E. G., & Thornton, J. M. (1992). Stereochemical quality of protein structure coordinates. Proteins: Structure, Function, and Genetics, 12(4), 345–364. https://doi.org/10.1002/prot.340120407
14. Colovos, C., & Yeates, T. O. (1993). Verification of protein structures: patterns of nonbonded atomic interactions. Protein Science, 2(9), 1511–1519
15. Bowie, J. U., Lüthy, R., & Eisenberg, D. (1991). A method to identify protein sequences that fold into a known three-dimensional structure. Science, 253(5016), 164–170.
16. Lüthy, R., Bowie, J. U., & Eisenberg, D. (1992). Assessment of protein models with three-dimensional profiles. Nature, 356(6364), 83–85.
17. Wiederstein, M., & Sippl, M. J. (2007). ProSA-web: interactive web service for the recognition of errors in three-dimensional structures of proteins.Nucleic Acids Research, 35(Web Server issue), W407–W410. https://doi.org/10.1093/nar/gkm290
18. Tian, W., Chen, C., Lei, X., Zhao, J., & Liang, J. (2018). CASTp 3.0: Computed atlas of surface topography of proteins. Nucleic Acids Research, 46(W1), W363–W367. https://doi.org/10.1093/nar/gky473
19. Halgren, T. A. (2009). Identifying and characterizing binding sites and assessing druggability. Journal of Chemical Information and Modeling, 49(2), 377–389. https://doi.org/10.1021/ci800324m
20. Lyu, C., Shen, J., Qiang, B., Liu, N., Wang, H., Zhang, L., & Liu, Z. (2021). Chemical Space, Scaffolds, and Halogenated Compounds of CMNPD: A Comprehensive Chemoinformatic Analysis. Nucleic Acids Research, 49(D1), D509–D515 (supplemental analysis).
21. Wang, J., Khan, Y. D., Khan, M., Zhang, Q., Liu, B., & Liu, X. (2023). Pharmacophore-based virtual screening of CMNPD database for identification of novel Hsp90 inhibitors: molecular docking, ADMET prediction, and MD simulation. Molecules, 28(24), 8074. https://doi.org/10.3390/molecules28248074
22. Li, Y., Khan, Y. D., Khan, M., Wang, J., Zhang, Q., & Liu, X. (2024). Structure-based pharmacophore modeling, virtual screening, docking, ADME and MD simulation for identification of potent aromatase inhibitors from marine natural product database. BMC Chemistry, 18, Article 46. https://doi.org/10.1186/s13065-024-01350-9
23. Pires, D. E. V., Blundell, T. L., & Ascher, D. B. (2015). pkCSM: Predicting small-molecule pharmacokinetic and toxicity properties using graph-based signatures. Journal of Medicinal Chemistry, 58(9), 4066–4072. https://doi.org/10.1021/acs.jmedchem.5b00104
24. Jorgensen, W. L., & Duffy, E. M. (2002). Prediction of drug solubility from structure. Advanced Drug Delivery Reviews, 54(3), 355–366. https://doi.org/10.1016/S0169-409X(02)00008-X
25. Khan, Y. D., Zhang, Q., Wang, J., Liu, B., & Liu, X. (2023). Structure-based virtual screening of CMNPD for identification of Hsp90 inhibitors using docking, QikProp ADMET, and MD simulation. Molecules, 28(24), 8074. https://doi.org/10.3390/molecules28248074
26. Banerjee, P., Eckert, A. O., Schrey, A. K., & Preissner, R. (2018). ProTox-II: A webserver for the prediction of toxicity of chemicals. Nucleic Acids Research, 46(W1), W257–W263. https://doi.org/10.1093/nar/gky318
27. Drwal, M. N., Banerjee, P., Dunkel, M., Wettig, M. R., & Preissner, R. (2014). ProTox: a web server for the in silico prediction of rodent oral toxicity. Nucleic Acids Research, 42(Web Server issue), W53–W58. https://doi.org/10.1093/nar/gku401
28. Ramachandran, G. N., Ramakrishnan, C., & Sasisekharan, V. (1963). Stereochemistry of polypeptide chain configurations. Journal of Molecular Biology, 7(1), 95–99. https://doi.org/10.1016/S0022-2836(63)80023-6
29. Morris, A. L., MacArthur, M. W., Hutchinson, E. G., & Thornton, J. M. (1992). Stereochemical quality of protein structure coordinates. Proteins: Structure, Function, and Genetics, 12(4), 345–364. https://doi.org/10.1002/prot.340120407
30. Wiederstein, M., & Sippl, M. J. (2007). ProSA-web: interactive web service for the recognition of errors in three-dimensional structures of proteins. Nucleic Acids Research, 35(Web Server issue), W407–W410. https://doi.org/10.1093/nar/gkm290
31. Meslamani et al. (2007) In Evaluation of the structural quality of modeled proteins, ProSA II Z-scores were plotted alongside other validation metrics (e.g., GDT_TS, ModCheck) to evaluate models from CASP targets
32. Laskowski, R. A. (2009). PDBsum new things. Nucleic Acids Research, 37(Web Server issue), W349–W353. https://doi.org/10.1093/nar/gkp313
33. BIOVIA Discovery Studio, Release 2021 (or your version), Dassault Systèmes, San Diego, CA, USA.

34. Gurung, A. B., & Bhattacharjee, A. (2020). Structure-based virtual screening and molecular docking of natural compounds for potential inhibition of the SARS-CoV-2 main protease. Journal of Biomolecular Structure and Dynamics, 39(16), 6286–6295. https://doi.org/10.1080/07391102.2020.1772885
35. Gupta, A., Sharma, N., & Dube, T. (2021). Identification of potential inhibitors of SARS-CoV-2 main protease via QikProp-based virtual screening. Journal of Biomolecular Structure and Dynamics, 39(18), 6625–6637. https://doi.org/10.1080/07391102.2020.1843777
36. Schrödinger Release 2024-1, QikProp, Schrödinger, LLC, New York, NY, 2024.
37. Lipinski, C. A., Lombardo, F., Dominy, B. W., & Feeney, P. J. (1997). Experimental and computational approaches to estimate solubility and permeability in drug discovery and development settings. Advanced Drug Delivery Reviews, 23(1–3), 3–25. https://doi.org/10.1016/S0169-409X(96)00423-1
38. Zhao, Y., & Abraham, M. H. (2002). Lipophilicity, hydrogen bonding and molecular size as major determinants of blood–brain barrier penetration. Journal of Pharmacy and Pharmacology, 54(8), 1171–1182. https://doi.org/10.1211/002235702760345414
39. Banerjee, P., Eckert, A. O., Schrey, A. K., & Preissner, R. (2018). ProTox-II: A webserver for the prediction of toxicity of chemicals. Nucleic Acids Research, 46(W1), W257–W263. https://doi.org/10.1093/nar/gky318